Report for Research Project 2:

ADAM17 and its potential role in Alzheimer's disease: establishing its detection through Western Blot

Mariana Pliego Caballero
(Biomedical Sciences Master Program)

Supervisor:

Prof. Ulrich L.M Eisel

Daily Supervisors:

Valentina Pegoretti, MSc

Natalia Ortí Casañ, MSc

Ate Boerema, PhD

August, 2018

Table of contents

ABSTRACT

Alzheimer's disease (AD) is a neurodegenerative disorder characterized by the presence of amyloid beta plaques and neurofibrillary tangles. In addition, neurodegeneration has been recognized as another important player in the development of the disease, mainly due to the release of proinflammatory factors that further promote tissue damage. Among this proinflammatory molecules, some evidence point out tumor necrosis factor-alpha (TNF-α) as a molecule with dual effects on the pathology of AD, depending if it acts as a soluble (sTNF-α) or membrane bound protein (tmTNF-α) and the receptor it binds to. While signaling through TNF Receptor 2 (TNFR2) seems to have protective effects, TNF Receptor 1(TNFR1) is mainly associated with detrimental effects. Since the tmTNF binds both TNFR1 and TNFR2, but the sTNF acts mostly through TNFR1, the ratio of sTNF-α / tmTNF-α is probably important to determine whether TNF-α participates in the pathology of Alzheimer's disease as a protective or detrimental molecule. ADAM17 is the metalloprotease involved in the cleavage of tmTNF-α to release sTNF-α. For this reason, we aimed to test if ADAM17 protein expression is increased in the brain of a mouse model of AD, thereby promoting an increased production of sTNF-α and signaling through TNFR1, further contributing to the pathology. Since we have not studied ADAM17 before, this project was mainly focused in establishing the conditions for its proper detection through Western Blot. There were several complications to detect ADAM17 in the blots and even though we probably managed to obtain bands that correspond to our protein of interest, we were not able to differentiate the bands that correspond to its mature and immature forms.

INTRODUCTION

Alzheimer's disease

Alzheimer's disease is a neurodegenerative disorder recognized as the most common cause of dementia in elderly people. Pathologically it is characterized by the presence of two major hallmarks: extracellular beta amyloid (Aβ) plaques and intracellular neurofibrillary tangles (NFT)(Rubio-Perez and Morillas-Ruiz, 2012).

The Aβ plaques are the result of the aggregation of a cleaved form of the amyloid precursor protein (APP). The physiological role of APP is not completely elucidated; however, APP is a target of proteolytic processing by three different kinds of proteases, α-, β-, and γ-secretases. When APP is sequentially cleaved by the α- and γ-secretase, the result is the production of three non-amyloidogenic peptides: a soluble ectodomain (sAPPα), the P3 peptide and the APP intracellular domain (AICD) (*Figure 1)*. On the other hand, when the APP is processed by the β- and γ-secretases, a soluble ectodomain (sAPPβ), the AICD and the Aβ peptide are released (Tomita, 2017). This last peptide most commonly has a length of 40 or 42 amino acids and tends to agglomerate forming oligomers, which are probably the most neurotoxic aggregate intermediates. Later these turn into larger structures and finally results in the formation of plaques (Jeong, 2017).

NFT are formed by hyper-phosphorylated Tau protein. Under normal conditions the Tau protein is essential for the structure and support of neurons since it regulates the assembly and stability of the microtubules of the neuronal axons. In AD however, the hyperphosphorylation of Tau results in the disengagement with the microtubules and due to the insolubility of the protein it self-aggregates forming paired helical filaments and eventually also NFT (Jeong, 2017; Raskin et al., 2015).

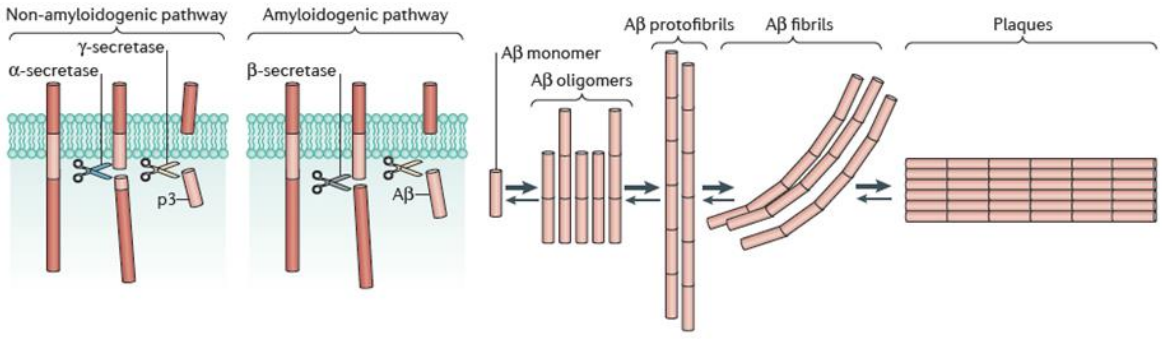

Figure 1 Proteolytically processing of the amyloid precursor protein APP. The non-amyloidogenic and amyloidogenic pathways are represented. In both, the upper peptide obtained after γ-secretase mediated cleavage represents the APP intracellular domain (AICD). ADAM17 and ADAM10 can act as α-secretases. Modified from (Heppner et al., 2015).

Neuroinflammation in Alzheimer's disease

Besides the Aβ plaques and NFT, another important player in the pathophysiology of AD is neuroinflammation; defined as the brain's immune response activation (Zhang and Jiang, 2015). This is characterized by diverse cellular and molecular changes, including the release of inflammatory factors mainly caused by the activation of microglia and astrocytes. As other inflammatory processes, the aim is to protect the tissue against infections, damage and injuries, however, when the first insult is not resolved, chronic inflammation contributes to tissue damage (Rubio-Perez and Morillas-Ruiz, 2012).

The central nervous system (CNS) is equipped with specific types of cells in charge of its protection: microglia and astrocytes. Microglia are innate immune cells that represent the first line of defense against pathogens and injury in the brain, since they are constantly surveying for damage and also provide support for the maintenance of the CNS. Astrocytes, on the other side, are supporting cells that perform several functions like production of trophic factors, regulation of neurotransmitters and ion homeostasis, additionally, as microglia also release inflammatory factors (Zhang and Jiang, 2015). In the AD pathology, on first instance, astrocytes and microglia play a neuroprotective role by promoting Aβ phagocytosis and clearance. However, upon persistent activation, the secretion of inflammatory factors like proinflammatory cytokines, chemokines, reactive oxygen species and proteases, further contribute to neuronal death. In addition, they promote the production of β-secretase, increasing the generation of Aβ and creating a feedback loop (Wang et al., 2015).

Among the molecules produced, Interleukin (IL)-6, IL-18, IL-12, IL-1 and tumor necrosis factor-alpha (TNF-α) have been recognized as major players in neuroinflammation in AD (Rubio-Perez and Morillas-Ruiz, 2012; Wang et al., 2015). TNF-α is a pro-inflammatory cytokine and signaling molecule with high impact on the regulation of the immune response. It is mainly produced by immune cells in response to a variety of stimuli like infections or tissue damage (Fischer et al., 2015; Probert, 2015; Tobinick, 2009). However, under certain circumstances TNF-α also contributes to pathophysiological processes like cancer, rheumatoid arthritis and neurodegenerative diseases (Dong et al., 2015).

Tumor necrosis factor-alpha

TNF-α is synthetized as a 26-KDa transmembrane protein (tmTNF-α) and is biologically active as a homotrimer. When proteolytically processed by the TNF-α converting enzyme (TACE), the soluble 17-KDa form of the protein is released (sTNF-α), which also acts as a trimer. Both tmTNF-α and sTNF-α exert their effects by binding with the transmembrane TNF-receptors (TNFR1 and TNFR2) which are differently expressed and regulated *(Figure 2).* For instance, while TNFR1 can be activated by both sTNF-α and tmTNF-α, TNFR2 is mainly activated by tmTNF-α (Dong et al., 2015; Fischer et al., 2015; Van Hauwermeiren et al., 2011; Montgomery and Bowers, 2012).

Despite the fact that the extracellular domains of the TNFRs are similar, the structure of their intracellular domains lacks homology (Fischer et al., 2015); this is reflected in the activation

of different signaling pathways and hence distinct actions. As a matter of fact, TNFR1 activation is mainly associated with the promotion of apoptosis and cytotoxicity, whereas TNFR2 activation is related with cell survival and protective functions (Fischer et al., 2015; Van Hauwermeiren et al., 2011). However, their complex signaling can have other effects, either opposite or complementary and this may depend on external factors like cell type and environment (Dong et al., 2015; Montgomery and Bowers, 2012).

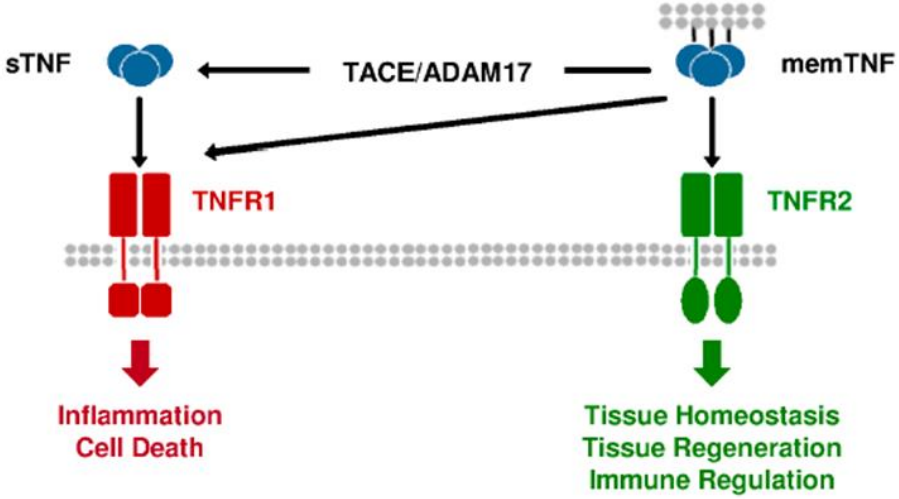

Figure 2 Activation of the TNFRs. While membrane bound TNF-α binds both receptors, TNFR1 and TNFR2, the soluble TNF-α mainly acts through the activation of TNFR1. The outcome of the activation of the receptors is also different, TNFR1-mediated signaling is associated with inflammation and cell death, in contrast TNFR2-mediated signaling is related with tissue homeostasis, regeneration and immune regulation. TACE/ ADAM17 is the enzyme in charge of releasing the soluble TNF-α after cleaving transmembrane TNFα. Modified from (Fischer et al., 2015).

Several research groups have found evidence supporting the participation of TNF-α in the pathology of AD. Genetic studies found an association of certain TNF-α and TNFRs single nucleotide polymorphisms with the risk of developing AD (Di Bona et al., 2009). At the protein level, expression of TNF-α was found to be increased in AD patients, this has been demonstrated in plasma and serum (Alvarez et al., 2007; Bruunsgaard et al., 1999; Fillit et al., 1991) as well as in brain tissue (Zhao et al., 2003). In addition a co-localization of TNF-α with plaques was observed in AD patients and in a mouse model of Alzheimer's (Benzing et al.). Mechanistically, TNF-α has also been shown to promote Aβ production by increasing the expression of the β-secretase gene (BACE) and the activity of γ-secretase (He et al., 2007; Liao et al., 2004) .

Interestingly, the effects of TNF-α on AD seem to differ depending on the activated receptor. For instance, protein levels of TNFR1 are increased in brains from AD patients whereas TNFR2 are decreased (Jiang et al., 2014; Zhao et al., 2003). In mouse models of the disease, deletion of either TNFR2 or both receptors results in exacerbation of the pathology, which can be reversed by overexpressing TNFR2 (Montgomery et al., 2011). On the contrary, deletion of only TNFR1 leads to a decreased Aβ production and prevents memory deficits (He et al.,

2007). In the same way, inhibition of sTNF-α, the preferred ligand for TNFR1, diminished the AD pathology (McAlpine et al., 2009). Overall, these results suggest that the activation of TNFR1 in AD is associated with detrimental effects, while TNFR2 activation may lead to beneficial protective effects.

TACE/ADAM17

As it was previously mentioned, sTNF-α is released with the cleavage of tmTNF-α mediated by TACE (Dong et al., 2015; Montgomery and Bowers, 2012). TACE, is a metalloprotease member of the family of the A disintegrin and metalloprotease (ADAM) enzymes, also known as ADAM17. There are around 40 ADAMs in the mammalian genome and while most of them possess an enzymatic activity and adhesive properties, others are not catalytically active. The importance of the proteolytic ADAMs relies on the fact that release of soluble molecules is a common biological mechanism involved in cell signaling. This explains why ADAM-mediated shedding influences a variety of processes such as intracellular communication, cell fate determination, migration, proliferation and immunity. In addition, they are also involved in pathophysiological conditions such as cancer and chronic inflammatory diseases.

ADAM17 is the most well-known member of the ADAMs, probably because it promotes the cleavage of more than 80 substrates, among which are receptors, growth factors, adhesion molecules and cytokines *(Table 1).* ADAM17 is expressed in several tissues including skeletal tissue, gonads, heart, kidney and the brain.

Table 1 ADAM17 Substrates

Cytokines, growth factors		Receptors		Adhesion molecules	Other molecules
TNF	SEMA4D	TNFR1	NPR	ICAM-1	APP
TGFα	LAG-3	TNFR2	HER4/ ErbB4	VCAM-1	GP
AREG	DLL1	p75NTR	Notch1	NCAM	CA9
EREG	KL1	IL-6Rα	TNFRSF8, CD30	ALCAM	PRNP, PrPc
EPNG, Epigen	KL-2	IL-1R2	TNFRSF5, CD40	L1-CAM	KL
NRG1, Heregulin	MICA	NTRK1, TrkA	GPIba	EpCAM	MUC-1
HB-EGF	MICB	GHR	GPV	DSG2	LYPD3, C4.4A
Pref1	Jagged	CSF1R, M-CSFR	GPVI	CD62L	VASN
CX3CL1	LTA	SORL1, SORL2	SDC1	Collagen XVII	CD163
TRANCE/RANKL	TMEFF2	SORCS1	SDC4	PVRL4, Nectin-4	PMEL17
CSF-1	FLT-3L	SORCS3	KDR, VEGFR2	CD44	
		SORT1	CD89	F11R, JAM-A	
		CD91/ APOER	Ptprz		
		PTPRF, PTP-LAR	IGF2-R		
		EPCR	M6P / IGF2R		
		ACE2			
		LOX-1			

From (Scheller J , 2011)

The domain structure of the ADAMs is conserved and specifically for ADAM17, it contains an N-terminal signal sequence, followed by a pro-domain, a metalloprotease domain, a disintegrin domain, a membrane proximal domain, a single transmembrane domain and a cytoplasmic tail *(Figure 3a)* (Xu et al., 2016; Zunke and Rose-John, 2017). The pro-domain inhibits the catalytic activity of ADAM17 and hence has to be removed before it can act on their ligands through a process of maturation. When ADAM17 is just synthetized it is stored at the rough endoplasmic reticulum, then it is transported to *trans*-Golgi network, where the pro-domain is removed by furin proteases. Finally, it is transported to the cell membrane to perform its sheddase functions. However, only a small portion of the mature ADAM17 is transported to the surface, while most of it is stored intracellularly *(Figure 3b)* (Lorenzen et al., 2016; Xu et al., 2016).

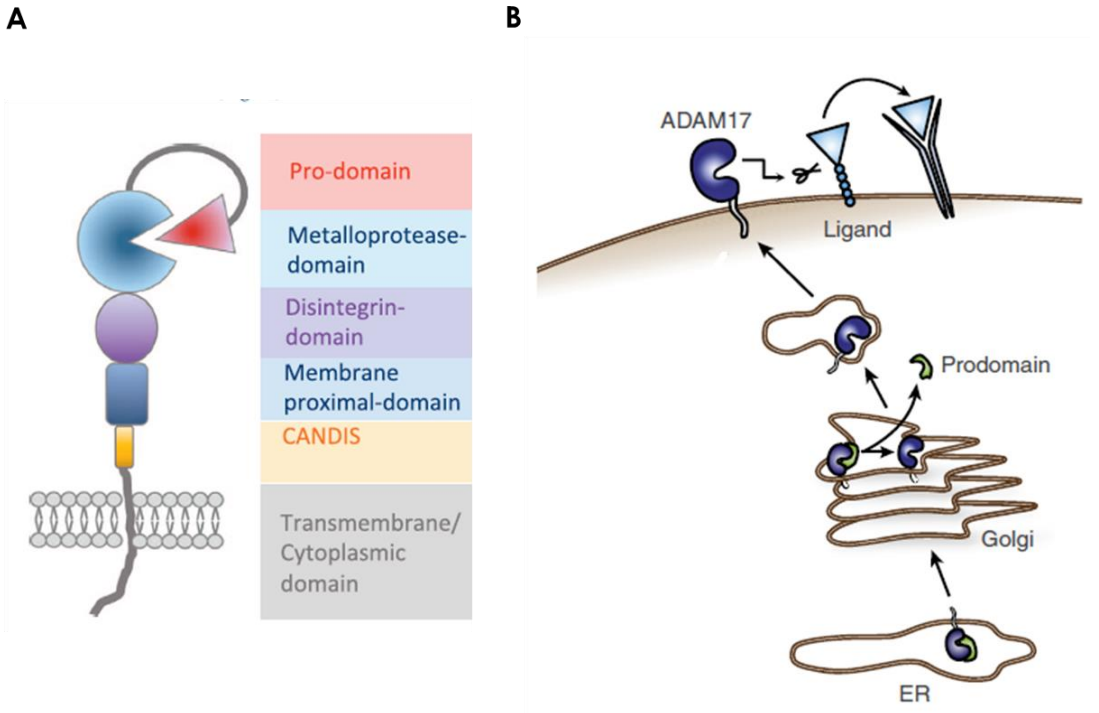

Figure 3 ADAM17 structure and processing. A: ADAM17 is a transmembrane protein with several domains: the pro-domain is present in the immature form of the protein and inhibits its activity by blocking the catalytic domain; the metalloprotease domain is responsible for the catalytic and shedding activity, the disintegrin, membrane proximal, CANDIS and cytoplasmic domains are involved in substrate recognition and regulation of the enzymatic activity. Modified from (Scheller J, 2011). B: After being synthetized in the Endoplasmic reticulum, ADAM17 is transported to the Golgi, where the prodomain is cleaved by furin proteases, once in its mature form it is transported to the cell surface to act as a sheddase. Modified from (Dombernowsky SL, 2015).

ADAM17-mediated shedding is involved in several biological processes; as a matter of fact ADAM17-knock-out mice are not viable, demonstrating the relevance of the factors it cleaves during development. Other processes on which ADAM17 participates include neurogenesis, immune response, angiogenesis, learning and memory. Interestingly, dysregulated function of

ADAM17 is also associated with pathological processes such as cancer, atherosclerosis, kidney fibrosis and psoriasis (Xu et al., 2016; Zunke and Rose-John, 2017).

Focusing on the topic of this project, TNF-α is the most known target of ADAM17, since the metalloprotease was first described and named after it was discovered to be responsible for the release of sTNF-α. Interestingly, ADAM17 is also responsible for the cleavage of its receptors, TNFR1 and TNFR2, which may act as a neutralizing mechanism for the TNF-α mediated signaling (Gooz, 2010; Scheller et al., 2011; Xu et al., 2016).

Hypothesis

Given that TNFR2 is preferentially activated through the tmTNF-α and that sTNF-α is a preferred ligand for TNFR1(Dong et al., 2015; Fischer et al., 2015), it seems plausible that an increased release of sTNF-α may lead to a higher activation of TNFR1. Therefore, we hypothesized that in the Alzheimer's brain, ADAM17 protein expression and activity is higher than in healthy brains, leading to an increased TNFR1-mediated signaling and further contributing to the pathology of AD.

Interestingly, ADAM17 along with its family member ADAM10 can act as α-secretases cleaving APP to produce the non-amyloidogenic sAPPα (Figure 1). The release of this peptide has been suggested to reduce the generation of Aβ and hence having a neuroprotective effect (Gooz, 2010; Xu et al., 2016; Zunke and Rose-John, 2017). In addition, ADAM17 has been observed to co-localize with plaques in brains from AD patients (Skovronsky et al., 2001). Although these observations may seem contradictory to our hypothesis, it may be possible that the presence of Aβ results in an increased expression of ADAM17 as a protective mechanism to compete with the β-secretase, but instead ends up contributing to the AD pathology through the release of sTNF-α. Hence, this further increases our interest in studying ADAM17 on the brain with Alzheimer's.

In order to test our hypothesis, we first aimed to analyze if the protein expression of ADAM17 was increased in the brains of J20 mice, a rodent model of the AD pathology. These transgenic mice overexpress the human APP gene with two mutations, promoting an Alzheimer's-like phenotype with a high production of Aβ and plaque development at a later age. As a methodological strategy, we decided to detect ADAM17 with the Western Blot technique.

MATERIALS AND METHODS

Animal tissue

For the immunodetection of ADAM17 performed with animal tissue; hippocampus, cortex, cerebellum, brainstem and rest brain of mice were employed. This tissue was dissected on December 2017 from C57BL/6J mice 17-21 months old, either wild type (WT) or J20. The dissected regions of the brain were placed in individual 1.5 mL tubes, snap frozen in liquid nitrogen and then stored at -20°C until the lysis protocol was performed.

Lysis of tissue

Hippocampus and cortex were lysed before the beginning of this project employing cytoskeletal extraction buffer (20 mM Tris-HCl pH 7.2, 150 mM NaCl, 2 mM MgCl2, 1% P40, 1mM dithiotreitol, 1 mM Na3VO4, 5mM NaF, 1mM PMSF and 1 µg/ml Leupeptin). Brainstems and rest brains were lysed employing a commercial RIPA buffer from Invitrogen (5mM Tris-HCl pH 7.6, 150mM NaCl, 1% NP-40, 1% sodium deoxycholate, 0.1% SDS). Cerebellums were processed at a different time point employing Triton X-100 lysis buffer (50 mM Tris-HCl pH 7.4, 150 mM NaCl, 1% Triton X-100). Regardless of the different composition of the buffers, a protease inhibitor and a phosphatase inhibitor tablet (Roche) were added just before the cell lysis. In addition, the metalloprotease inhibitor 1,10-phenanthroline was added to the Triton X-100 buffer in a final concentration 10 mM.

The dissected tissues were thawed on ice and kept cool during the whole process. Depending on the size of the tissue, 200-400 µL of the indicated lysis buffer were added along with a 1.5 mm pre-cooled stainless steel bead. The tubes were then powerfully shaken at 30 Hz, two times per 60 s with a Tissue lyser (Quiagen). Steel beads were removed and the samples were also homogenized with a sonicator at 70% potency, two times per 5 s. After shaking with the vortex for 10s, the samples were incubated for 30 min on the shaker and then spin down with a micro-centrifuge at 5°C for 45 min at 18,000 rpm. The supernatants were carefully collected on new tubes and pellets were discarded.

Cell culture

For experiments performed with cell cultures, HeLa and HEK293 cell lines were employed. This cell lines were already present at the laboratory under liquid nitrogen storage. The vial of HeLa was prepared and frozen on October 1997 and the one of HEK293 on October 2016. For the initiation of the culture, both cell lines were defrosted in thawing media (DMEM 25mM Glucose with 15 % FBS, 1% Penicillin and Streptomycin and 1% L-Glutamine). After a few days in culture, the media was switched to maintenance media (DMEM 25mM Glucose with 10% FBS, 1% Penicillin and Streptomycin and 1% L-Glutamine). Medium was renewed every 2-3 days and the cells sub-cultured weekly with a 1:5 to 1:20 ratio.

Cell lysis

For western blot experiments, 1 x 10^6 cells were seeded per well in a 6-well plate and grown for 2 days, then cells were quickly washed 2x with Dulbecco's Phosphate-Buffered Saline (DPBS) and 150 - 200µL of Triton X-100 (Tx) or RIPA lysis buffer were added and cells were then harvested with the use of a cell scrapper. In order to prevent the self-degradation of ADAM17, two metalloprotease inhibitors were added to the lysis buffer either in combination or alone and two different concentrations were tested, 1,10-phenanthroline (10mM or 20 mM) and BB-94 (1µM or 10µM). After harvesting, the cell lysates were frozen to -20°C until further processed. For this, lysates were thawed and kept all the time on ice, then samples were homogenized with a sonicator at 70% potency, two times per 5 s. After shaking with the vortex for 10s, the samples were incubated for 30 min on the shaker and then spin down with a micro-centrifuge at 5°C for 45 min at 18,000 rpm. The supernatants were carefully collected on new tubes.

For one experiment, pellets obtained after centrifugation were re-suspended in lysis buffer, samples were vortexed and also submitted to sonication in order to solubilize all the particles.

Electrophoresis and Western blot

Protein concentration of supernatants or pellets from both tissue and cell culture were determined with the Bradford protein assay. When possible, samples were diluted with lysis buffer to a concentration of 3µg/µL, otherwise all the samples from a same batch were diluted to the concentration of the sample with the minimum protein content.

Bio-Rad system

A single experiment was performed employing the electrophoresis and transfer system from Bio-Rad. For this step, samples were prepared by adding 19% SDS loading buffer with β-mercaptoethanol (25% of the buffer). Samples were then boiled at 96°C for 10 min just before loading the gels. A total of 35 µg of protein were loaded in 4-20 % TRIS-Glycine pre-cast gels. Electrophoresis was performed at 160 V for 15 min until samples reached the end of the stacking gel, then voltage was increased to 180 V for 30 min. Transfer was made on PVDF membranes (Immobilon P, Millipore) on a wet system with a 20% methanol buffer for 1.5h at 100 V.

Invitrogen system

For the rest of the experiments, the electrophoresis and transfer system from Invitrogen were employed. Samples were prepared by adding 25% LDS loading buffer and 10% reducing agent and then warmed up at 70°C for 10 min before loading the gels. Since the amount of protein loaded varied between experiments, this will be individually stated in the results section. Samples were run in 4-12% pre-cast Bis-TRIS gels for 45-60 min at 160 V. Transfer was made with the dry i-Blot system, program P2 7:30 min.

For both systems, after the transfer was finished, membranes were washed twice with Tris-buffered saline (TBS) (20 mM Tris-base and 150 mM NaCl) and two more times with TBS-T (20 mM Tris-base, 150 mM NaCl, 0.1% Tween-20). Afterwards, membranes were blocked either with i-Block, 0.2% in TBS-T or Bovine serum albumin (BSA) 2% in TBS-T for 1h at room temperature. Incubations with primary antibodies were performed over night at 4°C: anti-GAPDH from Thermofisher (MA1-16757), 1:3000 in iBlock; anti-ADAM17 from Abcam (ab2051) 1:500 – 1:1000 in iBlock or BSA (specific conditions stated under results); anti-ADAM17 from Santa Cruz Biotechnology (sc-390859) 1:500 in iBlock; anti-ADAM17 from Millipore (ABT94) 1:1000 in iBlock. The next day membranes were washed three times with TBS-T and then incubated 2h at room temperature with the appropriate secondary antibody: anti-rabbit IgG HRP-conjugated (Cell Signaling) 1:5000 or Goat anti-mouse IgG HRP-conjugated (Santa Cruz Biotechnology) 1:3000 for GAPDH and 1:5000 for ADAM17. After washing membranes three times with TBS-T and twice with TBS, detection was carried out with Pierce ECL substrate (Thermo scientific) and acquisition with the Chemidoc XRS imaging system (Bio-Rad).

When a stripping procedure was required, membranes were incubated for 15 min in a pre-warmed 65°C homemade stripping buffer (24 mM Glycine and 1.25% SDS in TBS-T, pH 2.0) at the roller-shaker, then buffer was exchanged for a fresh one and incubated for 15 min more, finally membranes were washed three times with TBS-T.

Image processing

The acquired images were processed using the software Image Lab from Bio-Rad (Version 5.2.1). Band intensities were calculated for the apparent mature, immature and degraded ADAM17, as well as for the loading control protein GAPDH. Intensity values for the different ADAM17 bands were normalized by diving them with the values of the respective loading control and then plotted.

RESULTS AND DISCUSSION

Standardization of ADAM17 antibody dilution

Since ADAM17 had not been studied before in our laboratory, an antibody for its detection was requested (ab2051 from Abcam) and thus the conditions for its proper use had to be standardized. With this purpose, on the first experiment three different dilutions (1:500, 1:1000, 1:2000) of the antibody were employed to select the one that best recognized our protein. Four different samples were employed: cortex from two transgenic mice carrying the wild type human APP (WT) and rest brain from two mice carrying a mutated version of the human APP (J20).

For this first experiment, electrophoresis was performed on a 4-20% TRIS/ Glycine gel with 35µg of protein per sample and transfer with a wet electroblotting on a polyvinylidene difluoride (PVDF) membrane. As it can be observed in *Figure 4,* several bands were visible on the blots, the most prominent located at the top of the gel and another one of ~160 KDa. Apart from that, on the cortex samples a smear was observed between ~65-55 KD and fainter bands were visible at ~150, 120, 90 and 60 KDa. Given that several bands were observed, we could not determine which one corresponded to the expected 93 KDa of ADAM17. However, since the same bands could be observed with the 1:500 and 1:1000 antibody dilution, we decided to keep using these concentrations for the following experiments, bands observed with the 1:2000 dilution were fainter.

Testing of different protein concentrations and samples of different species

The intense band observed at the top of the membrane of the first experiment seemed to indicate that proteins did not properly migrate through the gel and instead stayed between the stacking gel and the running gel. Since the employed 4-20% gradient gel should have a mesh with pores big enough to allow the migration of a 93 KDa protein like ADAM17, it is possible that the proteins were not properly denatured or reduced, avoiding their correct migration through the gel. For this reason, we decided to switch to Bis-Tris gels that make use

of a different procedure and reagents for denaturing and reducing. In addition, a dry transfer method was employed.

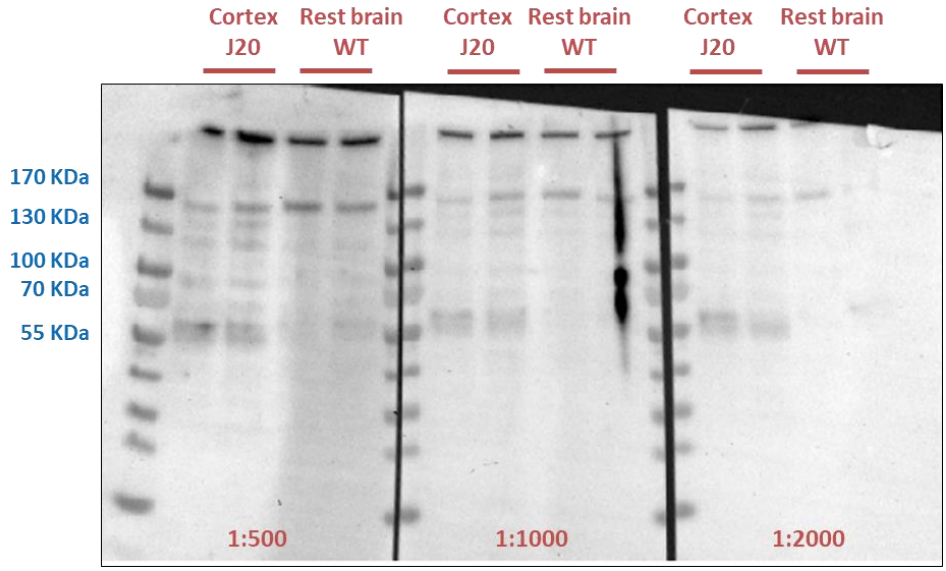

Figure 4 Standardization of the dilution of ADAM17 antibody. Samples from mice carrying a wildtype (WT) or mutated (J20) version of the human APP were run in a TRIS/ Glycine gel. 35µg of protein were loaded per sample.

We also tested two different protein concentrations (15 µg and 40 µg) in case the 35µg loaded in the previous experiment were not optimal for the detection of ADAM17. In addition, to compare whether some bands would be consistently observed regardless of the animal species, we also included two hamster samples and two samples from a human tumor. In *Figure 5* it can be observed that the top band and the one around 160 KDa present in the first experiment were not visible anymore. Instead, for the mice samples from cortex and rest brain, three bands were present at 140 KDa, 115 KDa and ~60 KDa. In addition, a more intense band of ~65 KDa is observed in the hamsters samples, which was also detected for two of the mice cortex samples. Regarding the amount of protein loaded, 15 µg did not seem to be enough to obtain sharp bands in the blot and some of them were not even visible. Surprisingly, human tumor samples resulted in the presence of several bands and, with exception to the 140 KDa and 115 KDa, the rest did not correspond to the observed bands with mouse or hamster tissue and even differed between the two human samples.

The protein sequence of the ADAM17 prodomain is expected to have a size of 22 KDa, which may explain the difference in size of the 140 KDa and 115 KDa bands observed, perhaps corresponding to the immature and mature forms of the protein, respectively. However, other research groups reported different sizes for the protein, making it complicated to confirm whether or not our antibody is detecting ADAM17; in addition the background of the blot is intense and, with exception to the human samples, the observed bands with the mouse and hamster tissue were not intense and sharp enough.

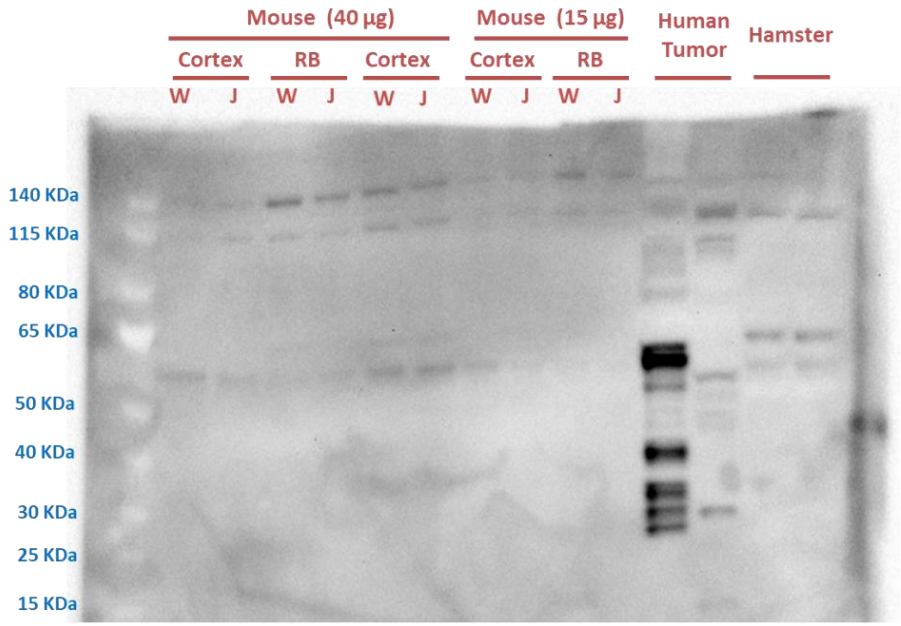

Figure 5 Effect of the variation of the protein content and origin of the sample on the detection of ADAM17. RB: rest brain, W: wild type, J: J20.

Addition of a metalloprotease inhibitor (1,10-phenanthroline)

In 2000, Schlöndorff et al. (Schlöndorff et al., 2000) performed western blot experiments to study the maturation of ADAM17 in COS-7 and THP-1 cells. When cell lysis was performed with a buffer containing the metalloprotease inhibitors 1,10-phenanthroline or BB-94, a band of ~100 KDa and another of ~80 KDa were observed after the incubation with different antibodies against ADAM17. In the absence of the inhibitors, however, the ~80 KDa band was weakly detected, while the ~100 KDa band remained unchanged, in addition a third band of ~60 KDa became visible in the blots. With these observations they concluded that the highest band represented the immature form of ADAM17, while the middle ~80 KDa was the mature form; the lowest band however represented a degraded form of the protein, result of the self-cleavage of ADAM17 cytoplasmic tail that occurred after cell lysis in the absence of metalloprotease inhibitors.

Given that the bands we observed with the ADAM17 antibody were faint and since other bands of a lower size were also present in the blots, being the most intense around ~60 KDa *(Figures 4 and 5)*, we thought our protein might being degraded during the lysis procedure. In order to test if this was the case, we lysed cerebellum tissue in the presence and absence of the metalloprotease inhibitor 1,10-phenanthroline. We expected to see a decrease in the intensity of the ~60 KDa band and an increase in the band observed around ~115 KDa. In addition, since samples were run in two different gels and transferred in separate membranes, we decided to test whether a different blocking agent would reduce the background observed on the previous blots. For this reason, one of the membranes was blocked with i-Block as before and the other with 2% BSA.

As previously, three different bands were observed on the blots, one around ~140 KDa, another at ~115 KDa and a lighter one at ~65 KDa *(Figure 6)*. Against our expectations, none of the bands showed a consistent intensity change in response to the presence of 1,10-phenanthroline, impeding us to determine again if we were actually detecting ADAM17. Regarding the blocking agent, the use of 2% BSA did not help to reduce the background but instead increased it, in addition, the blot seemed uneven with several dark spots in some regions. For this reason we continued using i-Block as the blocking agent.

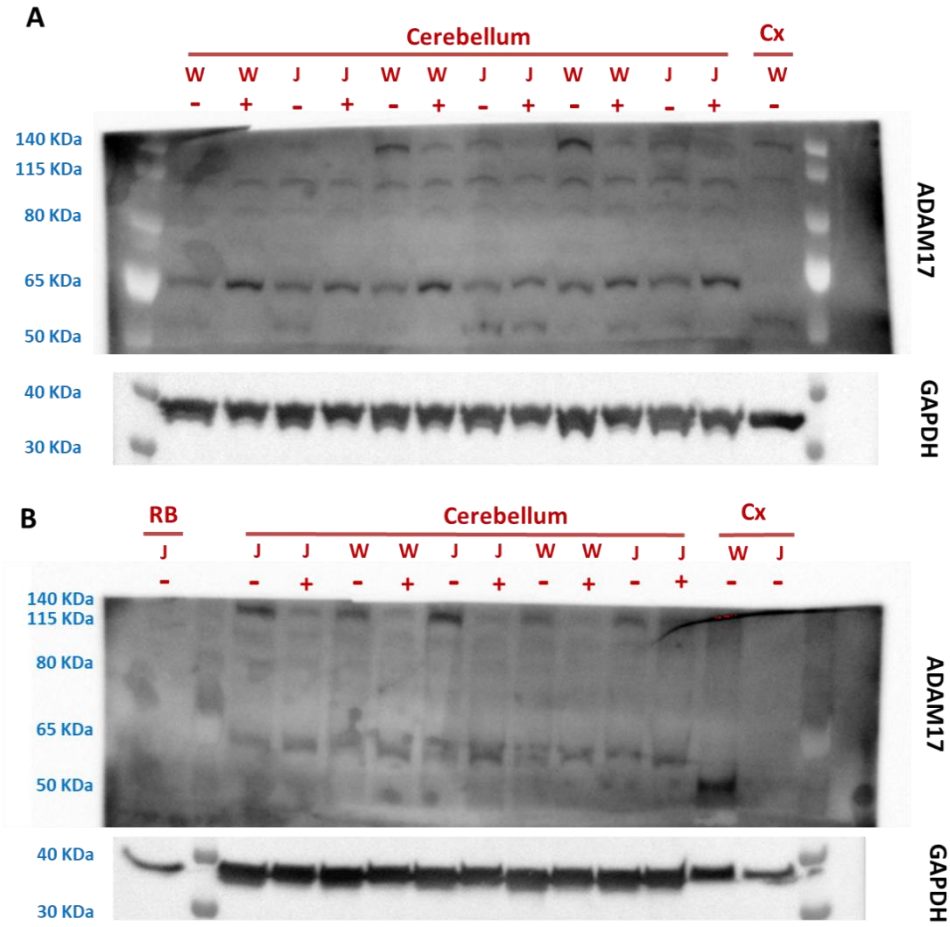

Figure 6 Effect of the addition of the metalloprotease inhibitor 1,10-phenanthroline. A. Blot incubated with i-Block as blocking agent. B. Blot incubated in 2 % bovine serum albumin. + and – denotes the presence and absence of the inhibitor on the lysis buffer. In addition to the cerebellum samples, rest brain (RB) and cortex (Cx) samples were loaded to compare the bands. W: wild type, J: J20 .

Use of cell lysates

The fact that no change on the intensity of the bands was observed in response to the addition of 1,10-phenanthroline, suggested us that perhaps ADAM17 was already degraded in the tissues employed for the experiments. Possibly for this reason the addition of protease inhibitor during the lysis of the tissue did not have any protective effect against degradation

anymore. Therefore, we decided to search for a positive control where the protein expression of ADAM17 had been reported; as a matter of fact, the provider of the antibody recommended to use a whole cell lysate from HeLa cells as a positive control for ADAM17. In addition, some research groups have detected this protein in the HeLa and HEK293 cells (Adrain et al., 2012; Lorenzen et al., 2016). Since both HeLa and HEK293 cell lines were available at our laboratory, we decided to employ these models to detect ADAM17 by Western blot and hence to obtain a positive control for our next experiments.

As a first aim, we wanted to test which of the fractions obtained after the centrifugation of the lysates contained ADAM17. For this purpose, both supernatants and pellets were employed for electrophoresis and western blot. In addition, several research groups that study ADAM17 report the use of Triton X-100 (Tx) lysis buffer, however for some of our previous experiments we employed RIPA buffer. For this reason, we decided to test whether differences in the composition of the buffer may be important for the detection of ADAM17. Finally, half of the obtained lysates were submitted to sonication whereas the other half did not receive it, with the purpose to test if this homogenization was necessary to improve the protein yield.

Protein quantification data did not show any difference in the amounts of protein obtained with or without sonication (*Table 2)*. However, differences in absorbance could be noticed between the different buffers, since values with RIPA buffer were higher than the ones obtained with Tx buffer with or without 1,10-phenanthroline. These results disagree with what can be observed in the blots, since the abundance of GAPDH was reduced for those cells lysed with RIPA buffer (*Figure 7a,b)* However, this could be given by an underestimation of the protein concentration of samples containing Tx buffer since triton X-100 interferes with the Bradford essay. Hence, when comparing samples prepared in different lysis buffers this should be taken into account.

Regarding the blots, in contrast to what we observed previously with the mice tissue, four different bands were visible with both HEK293 and HeLa cells. The highest band was ~115 KDa, followed by one of ~90 KDa, then two lower bands were present at ~65 KDa and a doublet at ~55 KDa *(Figure 7a,b)*. Interestingly the ~140 KDa band previously observed with tissue was not detected with the cell lysates. Concerning the use of 1,10-phenanthroline, the intensity of the 115 KDa and 90 KDa bands showed a tendency to be stronger when Tx buffer was supplemented with the metalloprotease inhibitor, however, this was rarely observed with the RIPA buffer that also contained the 1,10-phenanthroline *(Figure 7a-d)*. In addition, supposing that the 115 KDa and the 90 KDa bands corresponded to the immature and mature forms of ADAM17 respectively, no change in response to the inhibitor should be expected in the higher band since only the mature and active form of ADAM17 is subject to self-degradation. Finally, the ~65 KDa band, which we thought could correspond to the degraded ADAM17, seem to be reduced in response to 1,10 phenanthroline in the supernatants that did not receive sonication, while it was increased for those that received sonication. Hence, these results were intriguing and did not provide us with the answer we were expecting.

Table 2. Comparison of the absorbance and protein concentration in response to sonication

Sample	Absorbance	Conc.	Adjusted Conc.
HeLa Sup Tx	0.479	0.863	1.725
Hela Sup Tx + phe	0.523	1.387	2.773
HeLa Sup RIPA + phe	0.622	2.580	5.159
HeLa Sup Tx Son	0.513	1.272	2.545
Hela Sup Tx + phe Son	0.462	0.658	1.316
HeLa Sup RIPA +phe Son	0.605	2.375	4.749
HeLa Pell Tx	0.484	0.917	1.834
Hela Pell Tx + phe	0.491	1.007	2.014
HeLa Pell RIPA +phe	0.581	2.086	4.171
HeLa Pell Tx Son	0.481	0.887	1.773
Hela Pell Tx + phe Son	0.523	1.393	2.786
HeLa Pell RIPA +phe Son	0.561	1.845	3.689
HEK Sup Tx	0.481	0.881	1.761
HEK Sup Tx + phe	0.480	0.875	1.749
HEK Sup RIPA +phe	0.592	2.218	4.436
HEK Sup Tx Son	0.535	1.531	3.063
HEK Sup Tx + phe Son	0.469	0.742	1.484
HEK Sup RIPA + phe Son	0.580	2.073	4.147
HEK Pell Tx	0.569	1.947	3.894
HEK Pell Tx + phe	0.600	2.320	4.641
HEK Pell RIPA + phe	0.654	2.971	5.942
HEK Pell Tx Son	0.548	1.694	3.388
HEK Pell Tx + phe Son	0.622	2.586	5.171
HEK Pell RIPA +phe Son	0.603	2.357	4.713

Concentration values (Conc.) were obtained based on the calibration curve, adjusted concentration values (Adjusted Conc.) took into account the dilution factors employed to quantify the samples. Sup: supernatant, Pell: pellet, Tx: triton x-100 buffer, phe: 1,10-phenanthroline, son: sonication, HEK: HEK293 cells.

With respect to the difference between pellets and supernatants, it can be noticed that the 115 KDa and 90 KDa bands were barely visible on the pellets, on the contrary, the lower bands of 65 KDa and 55 KDa were more pronounced than in the supernatants *(Figure 7b,d)*. Two interesting differences can be observed between the employed lysis buffers: first, the 65 KDa band is much more intense for those cells lysed in Tx buffer with 1,10-phenanthroline and second, while for the Tx buffer with and without the inhibitor a doublet can be observed at 55 KDa, when lysis is performed with RIPA buffer, mainly a single upper band is detected. The reason of these differences is unknown for us. However, since ADAM17 is expected to have a size between 100 KDa to 80 KDa, and these bands are mainly visible on the supernatants, we decided to keep working only with this fraction of the lysates.

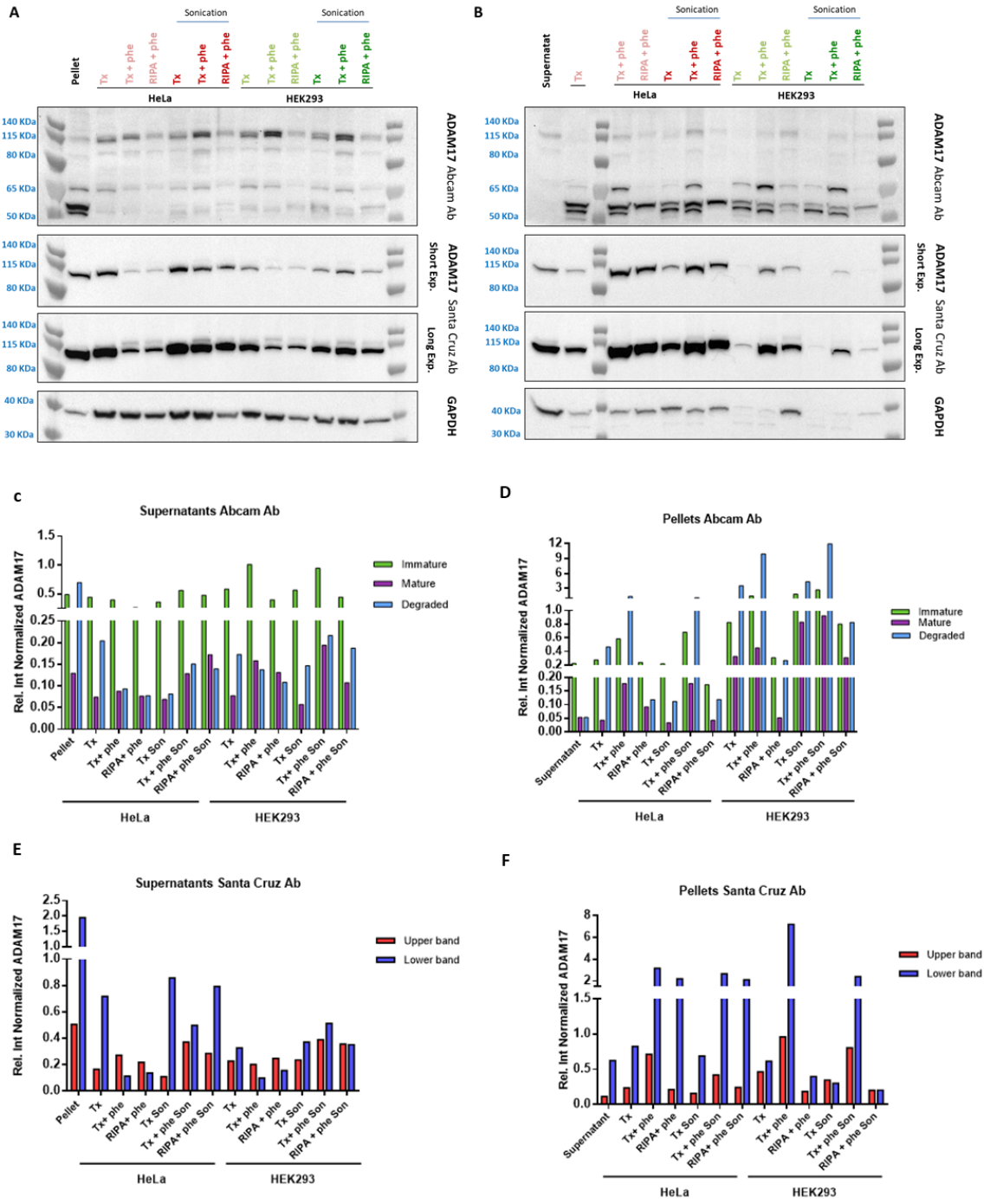

Figure 7 Test with protein extracts from cells in culture. A and B, Western blots for the detection of ADAM17 with two different antibodies: Abcam and Santa Cruz. For the second antibody, blots were developed with a short and a longer exposure (exp.) to observe the fainter bands. C-F. The normalized values of the different bands detected with the ADAM17 were plotted. C and D, for the Abcam antibody, the 115 KDa, 90 KDa and 60 KDa observed in the blots were denoted as immature, mature and degraded in the plots respectively. E and F, the band detected with the short exposure in the blot is denoted as upper, whereas the one observed only after the longer exposure is denoted as lower. Tx: Triton X-100 buffer, phe: 1,10- phenanthroline, Son: sonication.

Since all the experiments performed so far could not help us determine if the bands observed with the antibody employed actually corresponded to ADAM17, we decided to test an antibody from a different provider. The antibody anti-ADAM17 (B-6) from Santa Cruz is recommended for the detection of the immature form of the protein in human. Hence, we thought that using this antibody would help us determine if the 115 KDa band observed with the Abcam antibody corresponded to the immature form of ADAM17. For this purpose, the same blots were stripped with a low pH buffer and then re-probed with the mentioned antibody.

As it can be observed in *Figure 7a,b,* this antibody recognized a band of ~100 KDa that was not visible with the Abcam antibody; in addition, an upper band of ~115 KDa became visible with a longer exposure. Interestingly, the upper band was mainly visible in the presence of 1,10-phenanthroline, as for the lower band, differences in the intensity in response to the inhibitor were variable, sometimes being more intense and other fainter when compared to the Tx buffer *(Figure 7e,f)*. It can be noticed as well that the incubation with the Santa Cruz resulted in a cleaner blot than the ones obtained with the Abcam antibody, there was barely any background and only two bands were observed. However, given that no consistent difference was observed in response to the presence of the metalloprotease inhibitor, we could not determine yet if the bands corresponded to ADAM17 and if so, which one represented the mature form of the protein.

Use of a second inhibitor (BB-94)

Since the prospective ADAM17 bands showed no consistent change in their intensity in response to the addition of 1,10- phenanthroline to the lysis buffer, we considered testing the effect of BB-94, another metalloprotease inhibitor that has been reported to prevent the self-cleavage of ADAM17 (Schlöndorff et al., 2000). For this experiment, two different concentrations of 1,10-phenanthroline and BB-94 either alone or in combination were tested to study if any of these conditions could help to improve the detection of our protein of interest. In addition, all samples were run in duplicate in order to incubate half of them with the Abcam antibody and the other half with the Santa Cruz antibody. This approach was performed to confirm that the bands detected with the latter antibody in the previous experiment were not an artifact caused by an incomplete removal of the Abcam antibody during the stripping procedure.

In agreement with the previous experiment, an intense band of ~100 KDa and a fainter one of ~115 KDa were observed after incubation with the Santa Cruz antibody *(Figure 8a, c)*. Again the upper band was mostly visible in the presence of 1,10-phenanthroline but barely detected when lysis was performed on Tx buffer without inhibitors or when only BB-94 was added. Interestingly the intensity of the ~100 KDa band was lower when 20 mM 1-10, phenanthroline was present in the buffer. Regarding the antibody from Abcam, as previously, three bands are mainly detected: one at 65 KDa, another of 95 KDa and the heaviest of 115 KDa *(Figure 8b, d)*. For the latter band, this time it could be better appreciated that is not a

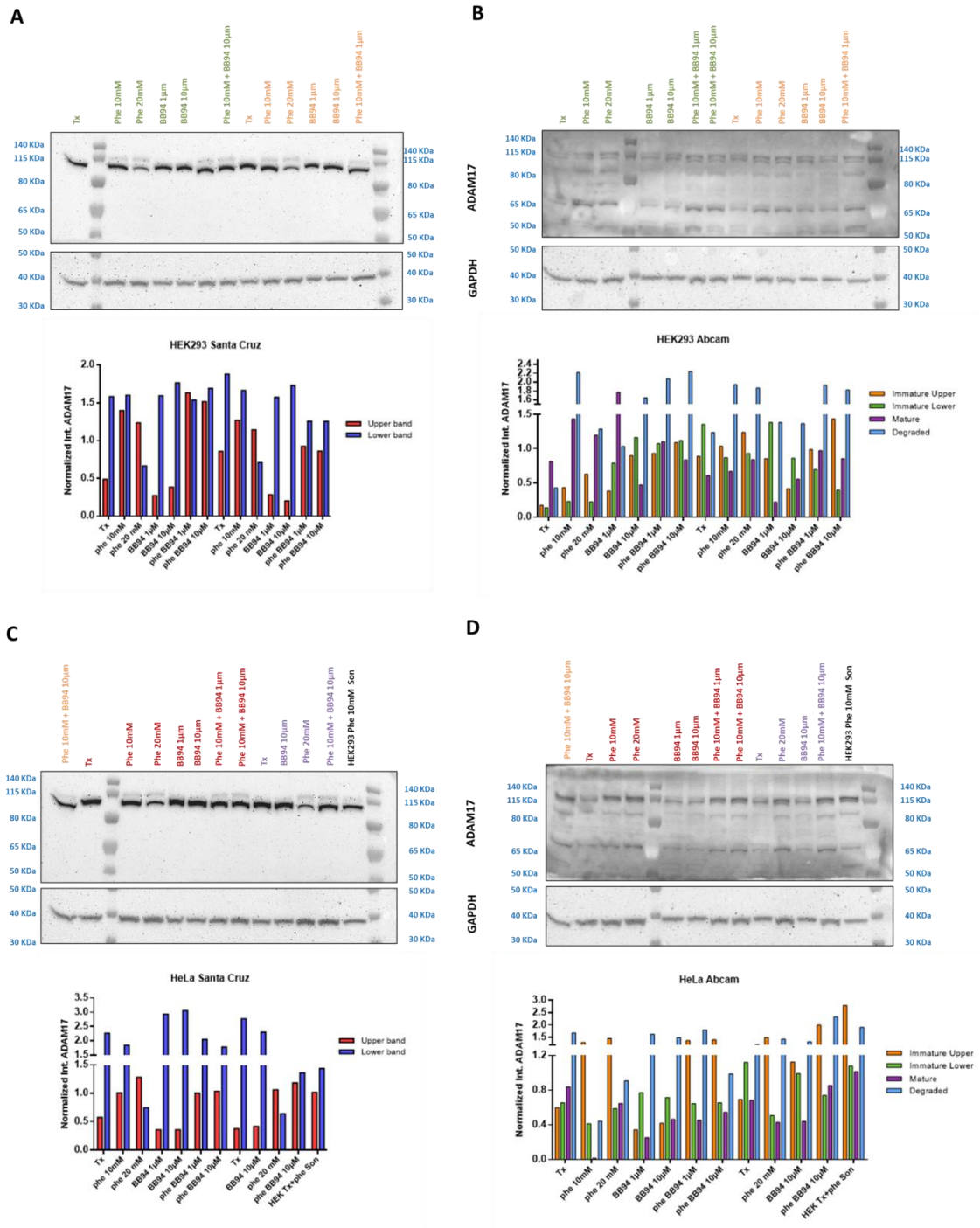

Figure 8 Test for the effect of a second metalloprotease inhibitor: BB-94. A and B, lysates from HEK293 cells; C and D, lysates from HeLa cells. B and D, for the Abcam antibody, the 115 KDa, 90 KDa and 60 KDa observed in the blots were denoted as immature, mature and degraded in the plots respectively. Tx: Triton X-100 buffer without inhibitors, phe: 1,10- phenanthroline, Son: sonication.

single band but a doublet and probably the lower part corresponds to the upper band detected by the Santa Cruz antibody. However, in none of the blots a consistent change in the intensity of the prospective mature ADAM17 bands was observed in response to the presence

of the inhibitors. In addition, the ~65 KDa band that we thought may be a degraded ADAM17 did not decreased in response to the inhibitors.

Use of a third antibody for ADAM17

The fact that we could not observe a consistent change in the abundance of the prospective mature or degraded bands in response to the presence of the metalloprotease inhibitors, made us wonder if this was due to the employed antibodies. First, for the the Santa Cruz antibody it was possible that only the immature form of ADAM17 was being detected. As a matter of fact, the provider recommends its use for the precursor form since the antibody was produced to target the first 300 amino acids (aa) of the protein and the propeptide spans the amino acids 18 to 214. Regarding the Abcam antibody, since all the blots obtained after performing incubations with it presented several bands and an intense background, we thought it was possible that the antibody was unspecific and was detecting other proteins besides ADAM17. If this was the case and the affinity for our protein of interest was not high, then we may had only partially detected the mature form of ADAM17.

Based on these possibilities, we decided to test a third antibody against ADAM17. This antibody is produced by Millipore and its use was recommended by Schöndorff and Blobel, the authors of the article where the self-cleavage of ADAM17 was reported for the first time. For this test, samples form HeLa and HEK293 cells obtained on the previous experiment were employed. In addition, two cerebellum samples from mice lysed with and without phenanthroline were included to compare if the bands obtained differed between tissue extracts and cell extracts. Finally, two samples from A431 cells, confirmed to express ADAM17 and purified prodomain were also included. These last samples were provided by another research group to act as a positive control.

As it can be observed in Figure 9, similar to the results obtained with the Abcam antibody, after incubation with the Millipore antibody several bands were detected, however the background was lighter and the bands sharper. In total seven bands were visible for the HeLa and HEK293 lysates, being the most prominent at ~115 KDa, ~90 KDa and a doublet of ~65 KDa, which seem to be in agreement with the bands observed with the Abcam antibody. Changes in the intensity of the bands were only visible when cells were lysed in the presence of phenanthroline, and both the prospective mature (~115 KDa) and immature (~90 KDa) forms of ADAM17 seemed increased. No changes were detected for the prospective degraded band. For the cerebellum lysates, only a doublet of ~70 KDa was clearly detected; as for the A431 lysates, one of the samples did not run properly on the gel probably by a defect on the well, but for the other sample, a band pattern similar to the HeLa and HEK293 was observed. Finally for the pro-domain, an intense smear of 70-80 KDa and a band of 65 KDa were present in the blot, however, this do not correspond to the prodomain since it has a size of ~25 KDa and that part of the membrane was not incubated with the antibody.

As before, when similar samples were incubated with the Santa Cruz antibody, the only observed changed was an increased intensity in the upper band in response to phenanthroline. Only a really dim band of 70 KDa could be observed for the cerebellum

samples after a long exposure. As expected, no bands were detected for the purified prodomain since the blot was cut on the lower part.

Altogether, since similar band patterns were obtained comparing the Abcam and the Millipore antibody, the results suggest that we are actually detecting ADAM17, however we are still not able to determine the band that correspond to the mature form of the protein. A possible reason to explain the lack of changes in response to the metalloprotease inhibitors, might be given by the protocol employed to obtain the protein samples. While we used total protein extracts, other research groups performed and additional step to enrich for glycoproteins and then used this fraction on the electrophoresis (Christova et al., 2013; Lorenzen et al., 2016; Schlöndorff et al., 2000; Schwarz et al., 2013; Sommer et al., 2016; Xu et al., 2012). This was done because ADAM17 is post-transcriptionally modified to acquire N-Glycans (Adrain et al., 2012; Schlöndorff et al., 2000). Therefore, it is possible that a low abundance of the protein in our extracts, results in a poor detection of the mature ADAM17. This could be tested by employing concanavalin A coated beads to purify glycoproteins.

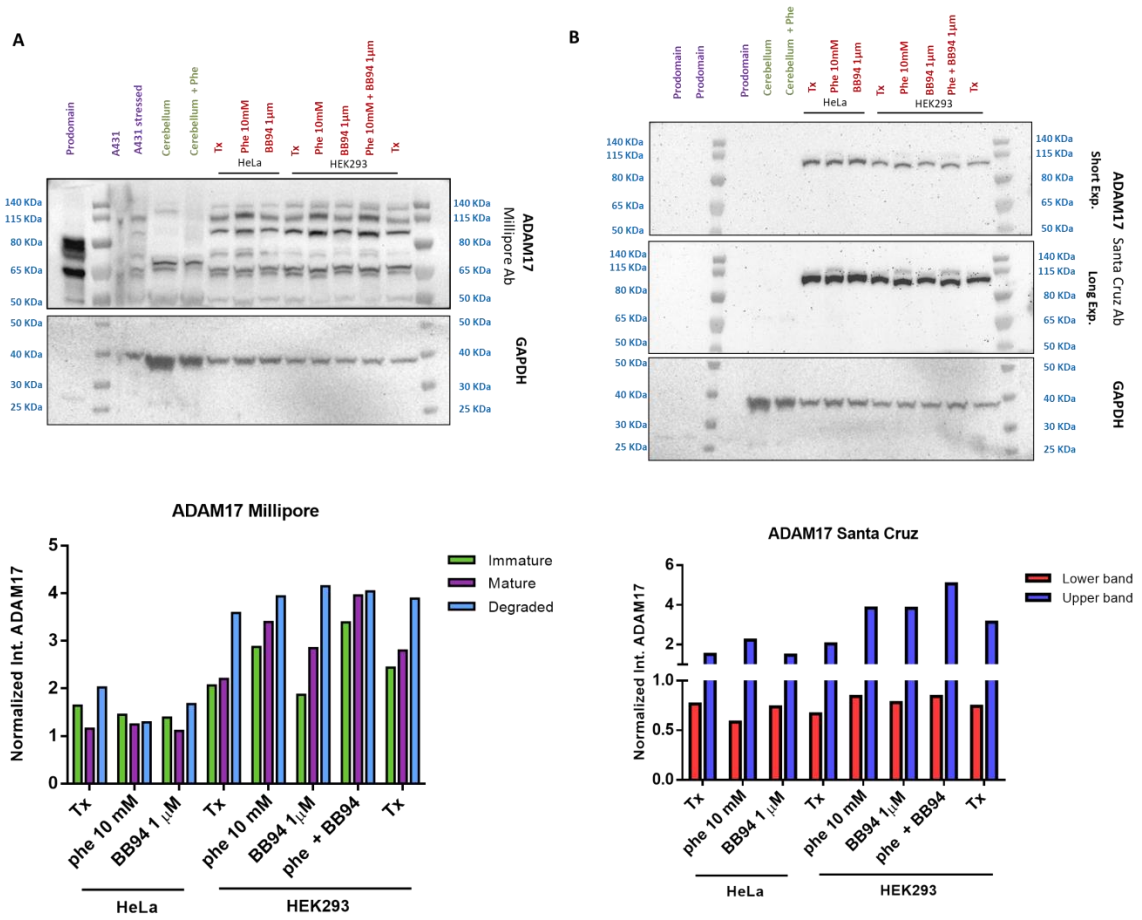

Figure 9 Use of a third antibody for ADAM17. A: Blot obtained after incubating with the Millipore antibody. The 115 KDa, 90 KDa and 65 KDa observed in the blots were denoted as immature, mature and degraded in the plots respectively B: Blot obtained after incubating with the the Santa Cruz antibody.. Tx: Triton X-100 buffer without inhibitors, phe: 1,10- phenanthroline. Amounts of protein loaded: HEK293 and HeLa lysates, 16.64 µg; Cerebellum, 18µg; A431, ~2µg; Prodomain, high concentration (purified).

An important point to be mentioned regarding the literature search performed for the current project, concerns the ambiguity of the ADAM17 protein size. Even though there are several articles showing western blots for this protein, the weights reported often differ, both for the precursor and the mature ADAM17 *(Table 3).* The reasons of the differences are not stated, however, they may be given by post-translational modifications. Once ADAM17 is synthetized, N-Glycans are added at the endoplasmic reticulum, then the protein is transported to the trans-Golgi, where the glycans are further modified (Adrain et al., 2012; Schlöndorff et al., 2000). In addition, the cytoplasmic region of ADAM17 can be phosphorylated, while the consequences of this modification are still debatable (Grötzinger et al., 2017), this could further contribute to the changes in the size of the protein. Overall these differences in the reported size of ADAM17, also contributed to the difficulty to determine if we were detecting the mature and immature forms of the metalloprotease.

Factors to take into consideration and future directions

Regardless our lack of success to determine if ADAM17 was detected by the tested antibodies, it is important to mention that once a proper protocol is established and it is possible to distinguish the immature and mature forms of the protein, results should be carefully examined. While the main goal of the present project was to determine whether ADAM17 protein levels are increased in a mouse model of AD, it is possible that the expression of the protein remains unchanged. However, this may not necessarily mean that ADAM17 is not involved in sTNF-α mediated signaling in the Alzheimer's pathology.

ADAM17 mediated shedding needs to be regulated to ensure it only takes place when needed. Interestingly, some groups have found an increased enzymatic activity is response to certain stimuli, without showing changes in the abundancy of the protein (Lorenzen et al., 2016; Sommer et al., 2017), suggesting that regulation of its activity is independent of its synthesis. As a matter of fact, several mechanisms are involved in controlling the activity of this important protease. For instance and as previously mentioned, ADAM17 is synthetized as an immature form that contains a prodomain, this keeps the metalloprotease inactive until it is transported to the Golgi, where furin proteases cleave the prodomain *(Figure 3)*.

Furthermore, for ADAM17 to act as a sheddase, it has to be present at the cell surface and this seems to be tightly regulated since only a small fraction of the protease is present at the membrane and the rest is stored intracellularly. Once in the membrane, ADAM17 is subject of other levels of regulation, for example, integrins can bind to its disintegrin domain resulting in the inhibition of its enzymatic activity (Grötzinger et al., 2017). Dimerization also results in ADAM17 inactivation, this because it facilitates its interaction with the tissue inhibitor of metalloproteases-3 (TIMP3), a well know inhibitor of other ADAMs which binds to the catalytic site of the protein with high affinity *(Figure 10)* (Xu et al., 2012).

Table 3 Different molecular weights reported for ADAM17 protein

Immature (KDa)	Mature (KDa)	Model used	Antibody	Reference
Not mentioned	93	Rat brain (cortex and hippocampus)	Abcam	(Zhao et al., 2003)
130 250 (dimer)		Cα and HeLa cells	QED Bioscience	(Xu et al., 2012)
~120	~95	MEF and embryonic extracts from mouse	Abcam Ab39162	(Christova et al., 2013)
160 (dimer)	75	Rat Cortex	QED Bioscience	(Bilousova et al., 2015)
~110	~80	Hippocampus mouse	Abcam Ab2051	(Corbett et al., 2015)
~ 120	95	MEFs, RAW264.7 macrophages, HEK293ET	Abcam Ab39162	(Cavadas et al., 2017)
120	100	THP-1 and COS-7 cells	Several non-commercial Ab	(Schlöndorff et al., 2000)
~ 120	95	MEFs	Non-commercial Ab	(Sommer et al., 2016)
~120	80	HEK293 , HeLa	Non-commercial Ab	(Lorenzen et al., 2016)
~120	90	HEK293 ET , HeLa	TACE (Ab39162)	(Adrain et al., 2012)
100	75	MDA-MB-231	R&D Systems MAB9301 (For non-reducing conditions)	(Dang et al., 2013)
130	100	ADAM17 $^{ex/ex}$ MEF transfected with ADAM17	Clone 10.1 Pineda Antikörper-Service and K133 non-commercial	(Schwarz et al., 2013)
~130	~100	MDA-MB-231 and MEFs	Abcam (ab39162 and ab2051), R&D Systems (MAB9301)	(Dombernowsky et al., 2015)
~130	~100	HUVECs	Chemicon AB19027	(Sommer et al., 2017)
~115	~90	MEFs, splenocytes (SPL) or bone marrow-derived macrophages form mice	Abcam ab39162	(McIlwain et al., 2012)

~ Denotes an approximate size, if it was not textually stated in the article.

In addition it has been recently emphasized that two different activities of ADAM17 must be distinguished: the catalytic activity and the shedding activity. The first one relates to its ability to cut small soluble peptides through the use of its catalytic domain, while the second refers to the release of membrane bound substrates; an activity that relies on ADAM17's ability to reach the membrane due to its flexible structure (Grötzinger et al., 2017; Sommer et al., 2016). As it can be deduced, some regulatory mechanisms inhibit ADAM17 at the catalytic level, while some others only control the shedding activity.

As an example of the latter, the membrane proximal domain (MPD) participates in ADAM17 activity regulation, through changes on its structure *(Figure 10)*. While an open conformation renders it flexible enough to reach the membrane, a closed conformation is stiff and unable to cleave membrane bound substrates. This conformational change can be promoted by the protein disulfide isomerase (PDI)(Grötzinger et al., 2017). Interestingly, the MPD was recently shown to couple ADAM17 activating stimuli to the interaction with its ligands. In response to signaling pathways, the phosphatidylserine phospholipids translocate from the inner to the outer leaflet of the membrane; with this exposure the MPD is able to interact with them and brings the catalytic site of ADAM17 closer to the cell surface and hence to its membrane bound ligands (Sommer et al., 2016).

Altogether these mechanisms demonstrate the complexity of ADAM17 and how results obtained from its study have to be carefully analyzed and complemented with different essays before jumping to conclusions. As an example, some research groups measure the activity of ADAM17 with the use of fluorogenic peptides. These enzymatic essays are based on the use of soluble peptides containing a fluorophore and a quencher, which are added to the culture media of cells, once ADAM17 cuts the peptides, the quencher is released and the fluorescence can be detected. Then, changes in the fluorescence are interpreted as changes in the enzymatic activity (Cavadas et al., 2017; Dombernowsky et al., 2015). However, when studying the physiological roles of ADAM17, these assays may not give a full answer, since an increased enzymatic activity does not necessarily mean that the shedding activity is also increased. For this reason, this first essay is usually complemented with the assessment of the shedding activity *in vitro* by transfecting cells with modified ADAM17 substrates fused to the alkaline phosphatase (AP). After stimulating the cells, supernatants are collected and the AP activity in the presence of its substrate is measured and represents the shedding activity of ADAM17 (Cavadas et al., 2017; Dombernowsky et al., 2015; Sommer et al., 2016, 2017).

Although this latter assay is a very informative strategy to assess the actual shedding activity of ADAM17, it poses two disadvantages for our research question: first, it is performed on cells in culture, while we aim to study brain tissue and second, it is tested in response to an added stimulus and we are studying a pathological situation. A possible way to overcome these difficulties may be through the co-immunoprecipitation of ADAM17 and mTNF-α. Since we hypothesize that in the AD brains ADAM17-mediated TNF-α release is augmented, then an increase interaction between these proteins would be needed and hence an increased co-immunoprecipitation may be observed. However, it is also possible that we will not even be able to detect this interaction given that enzymatic reactions are usually quick.

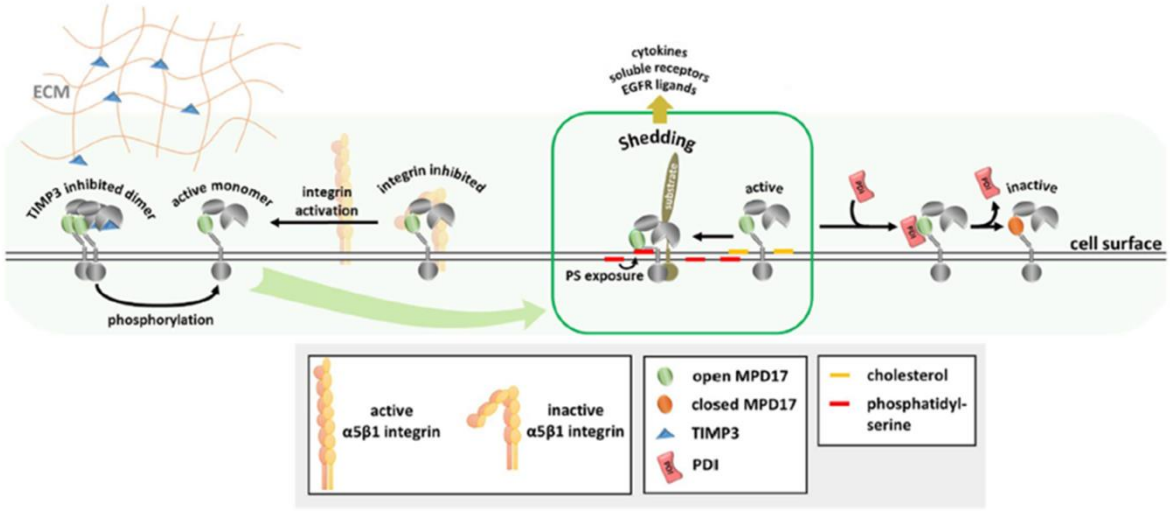

Figure 10 Regulatory mechanisms of ADAM17 shedding activity at the membrane. ADAM17 with its open membrane proximal domain (MPD) is activatable and the shedding process can be induced by exposure of phosphatidylserine in the outer leaflet of the cell membrane (depicted in the middle). However, this form of ADAM17 can be reversibly inhibited by its interaction with integrins or by its dimerization with subsequent TIMP3 binding (depicted on the left). On the other hand, PDI-mediated isomerization converts the open MPD isoform into the closed one which corresponds to the inactive form of ADAM17 (depicted on the right). From (Grötzinger, J 2017).

Regardless of this possibility, it would be worth it to perform the co-immunoprecipitations and test whether or not the interaction between ADAM17 and TNF-α can be detected. However, before being able to stablish a co-immunoprecipitation protocol for our protein of interest, we must assure that we can properly detect it through western blot and distinguish its mature and immature forms. Since we obtained sharp and intense bands with the Santa Cruz and Millipore antibodies, but we could not determine whether these corresponded to the mature form of ADAM17. A possible way to asses this is through the incubation of the protein extracts with furin, a protease known to cleave the prodomain of ADAM17 and compare the bands obtained before and after the addition of the enzyme (Schwarz et al., 2013). Then, if the Santa Cruz antibody is detecting the mature form of ADAM17, its detection should be increased with the furin treatment On the other hand, if the antibody only detects the immature form, the observed band should disappear in response to the cleavage caused by the enzyme.

In addition, to confirm the specificity of the employed antibodies a knockdown or knockout of ADAM17 could be performed through the use of siRNAs or CRISPR-Cas. All these essays in sum would help us to set-up a protocol in our lab for the detection of the mature form of ADAM17, to obtain a positive and negative control for its use in western blot and to establish the basis for other essays that could be useful for our research question.

REFERENCES

Adrain, C., Zettl, M., Yonka, C., Taylor, N., and Freeman, M. (2012). Tumor Necrosis Factor Signaling Requires iRhom2 to Promote Trafficking and Activation of TACE. Science (80-.). *335*, 225–228.

Alvarez, A., Cacabelos, R., Sanpedro, C., García-Fantini, M., and Aleixandre, M. (2007). Serum TNF-alpha levels are increased and correlate negatively with free IGF-I in Alzheimer disease. Neurobiol. Aging *28*, 533–536.

Benzing, W.C., Wujek, J.R., Ward, E.K., Shaffer, D., Ashe, K.H., Younkin, S.G., and Brunden, K.R. Evidence for glial-mediated inflammation in aged APP(SW) transgenic mice. Neurobiol. Aging *20*, 581–589.

Bilousova, T., Taylor, K., Emirzian, A., Gylys, R., Frautschy, S.A., Cole, G.M., and Teng, E. (2015). Neurobiology of Disease Parallel age-associated changes in brain and plasma neuronal pentraxin receptor levels in a transgenic APP / PS1 rat model of Alzheimer â€™ s disease. *74*, 32–40.

Di Bona, D., Candore, G., Franceschi, C., Licastro, F., Colonna-Romano, G., Cammà, C., Lio, D., and Caruso, C. (2009). Systematic review by meta-analyses on the possible role of TNF-alpha polymorphisms in association with Alzheimer's disease. Brain Res. Rev. *61*, 60–68.

Bruunsgaard, H., Andersen-Ranberg, K., Jeune, B., Pedersen, A.N., Skinhøj, P., and Pedersen, B.K. (1999). A high plasma concentration of TNF-alpha is associated with dementia in centenarians. J. Gerontol. A. Biol. Sci. Med. Sci. *54*, M357-64.

Cavadas, M., Oikonomidi, I., Gaspar, C.J., Burbridge, E., Badenes, M., Félix, I., Bolado, A., Hu, T., Bileck, A., Gerner, C., et al. (2017). Phosphorylation of iRhom2 Controls Stimulated Proteolytic Shedding by the Metalloprotease ADAM17/TACE. Cell Rep. *21*, 745–757.

Christova, Y., Adrain, C., Bambrough, P., Ibrahim, A., and Freeman, M. (2013). Mammalian iRhoms have distinct physiological functions including an essential role in TACE regulation. EMBO Rep. *14*, 884–890.

Corbett, G.T., Gonzalez, F.J., and Pahan, K. (2015). Activation of peroxisome proliferator-activated receptor α stimulates ADAM10-mediated proteolysis of APP. PNAS *112*, 8445–8450.

Dang, M., Armbruster, N., Miller, M.A., Cermeno, E., Hartmann, M., Bell, G.W., Root, D.E., Lauffenburger, D.A., Lodish, H.F., and Herrlich, A. (2013). Regulated ADAM17-dependent EGF family ligand release by substrate-selecting signaling pathways. Proc. Natl. Acad. Sci. *110*, 9776–9781.

Dombernowsky, S.L., Samsøe-Petersen, J., Petersen, C.H., Instrell, R., Hedegaard, A.M.B., Thomas, L., Atkins, K.M., Auclair, S., Albrechtsen, R., Mygind, K.J., et al. (2015). The sorting protein PACS-2 promotes ErbB signalling by regulating recycling of the metalloproteinase ADAM17. Nat. Commun. *6*.

Dong, Y., Dekens, D., De Deyn, P., Naudé, P., and Eisel, U. (2015). Targeting of Tumor Necrosis Factor Alpha Receptors as a Therapeutic Strategy for Neurodegenerative Disorders.

Fillit, H., Ding, W.H., Buee, L., Kalman, J., Altstiel, L., Lawlor, B., and Wolf-Klein, G. (1991). Elevated circulating tumor necrosis factor levels in Alzheimer's disease. Neurosci. Lett. *129*,

318–320.

Fischer, R., Kontermann, R.E., and Maier, O. (2015). Targeting sTNF/TNFR1 Signaling as a New Therapeutic Strategy. Antibodies *4*, 48–70.

Gooz, M. (2010). ADAM-17: The enzyme that does it all. Crit. Rev. Biochem. Mol. Biol. *45*, 146–169.

Grötzinger, J., Lorenzen, I., and Düsterhöft, S. (2017). Molecular insights into the multilayered regulation of ADAM17: The role of the extracellular region. Biochim. Biophys. Acta - Mol. Cell Res. *1864*, 2088–2095.

Van Hauwermeiren, F., Vandenbroucke, R.E., and Libert, C. (2011). Treatment of TNF mediated diseases by selective inhibition of soluble TNF or TNFR1. Cytokine Growth Factor Rev. *22*, 311–319.

He, P., Zhong, Z., Lindholm, K., Berning, L., Lee, W., Lemere, C., Staufenbiel, M., Li, R., and Shen, Y. (2007). Deletion of tumor necrosis factor death receptor inhibits amyloid β generation and prevents learning and memory deficits in Alzheimer's mice. J. Cell Biol. *178*, 829–841.

Heppner, F.L., Ransohoff, R.M., and Becher, B. (2015). Immune attack : the role of inflammation in Alzheimer disease. Nat. Publ. Gr. *16*, 358–372.

Jeong, S. (2017). Molecular and Cellular Basis of Neurodegeneration in Alzheimer's Disease. Mol. Cells *40*, 613–620.

Jiang, H., He, P., Xie, J., Staufenbiel, M., Li, R., and Shen, Y. (2014). Genetic deletion of TNFRII gene enhances the Alzheimer-like pathology in an APP transgenic mouse model via reduction of phosphorylated IκBα. Hum. Mol. Genet. *23*, 4906–4918.

Liao, Y.-F., Wang, B.-J., Cheng, H.-T., Kuo, L.-H., and Wolfe, M.S. (2004). Tumor necrosis factor-alpha, interleukin-1beta, and interferon-gamma stimulate gamma-secretase-mediated cleavage of amyloid precursor protein through a JNK-dependent MAPK pathway. J. Biol. Chem. *279*, 49523–49532.

Lorenzen, I., Lokau, J., Korpys, Y., Oldefest, M., Flynn, C.M., Künzel, U., Garbers, C., Freeman, M., Grötzinger, J., and Düsterhöft, S. (2016). Control of ADAM17 activity by regulation of its cellular localisation. Sci. Rep. *6*, 1–13.

McAlpine, F.E., Lee, J.K., Harms, A.S., Ruhn, K.A., Blurton-Jones, M., Hong, J., Das, P., Golde, T.E., LaFerla, F.M., Oddo, S., et al. (2009). Inhibition of soluble TNF signaling in a mouse model of Alzheimer's disease prevents pre-plaque amyloid-associated neuropathology. Neurobiol. Dis. *34*, 163–177.

McIlwain, D.R., Lang, P.A., Maretzky, T., Hamada, K., Ohishi, K., Maney, S.K., Berger, T., Murthy, A., Duncan, G., Xu, H.C., et al. (2012). iRhom2 Regulation of TACE Controls TNF-Mediated Protection Against Listeria and Responses to LPS. Science (80-.). *335*, 229–233.

Montgomery, S.L., and Bowers, W.J. (2012). Tumor necrosis factor-alpha and the roles it plays in homeostatic and degenerative processes within the central nervous system. J. Neuroimmune Pharmacol. *7*, 42–59.

Montgomery, S.L., Mastrangelo, M.A., Habib, D., Narrow, W.C., Knowlden, S.A., Wright, T.W.,

and Bowers, W.J. (2011). Ablation of TNF-RI/RII expression in Alzheimer's disease mice leads to an unexpected enhancement of pathology: Implications for chronic pan-TNF-α suppressive therapeutic strategies in the brain. Am. J. Pathol. *179*, 2053–2070.

Probert, L. (2015). TNF and its receptors in the CNS: The essential, the desirable and the deleterious effects. Neuroscience *302*, 2–22.

Raskin, J., Cummings, J., Hardy, J., Schuh, K., and Dean, R.A. (2015). Neurobiology of Alzheimer ' s Disease : Integrated Molecular , Physiological , Anatomical , Biomarker , and Cognitive Dimensions. 712–722.

Rubio-Perez, J.M., and Morillas-Ruiz, J.M. (2012). A review: Inflammatory process in Alzheimer's disease, role of cytokines. Sci. World J. *2012*.

Scheller, J., Chalaris, A., Garbers, C., and Rose-John, S. (2011). ADAM17: A molecular switch to control inflammation and tissue regeneration. Trends Immunol. *32*, 380–387.

Schlöndorff, J., Becherer, J.D., and Blobel, C.P. (2000). Intracellular maturation and localization of the tumour necrosis factor a convertase (TACE). Biochem. J. *347*, 131–138.

Schwarz, J., Broder, C., Helmstetter, A., Schmidt, S., Yan, I., Müller, M., Schmidt-Arras, D., Becker-Pauly, C., Koch-Nolte, F., Mittrücker, H.W., et al. (2013). Short-term TNFα shedding is independent of cytoplasmic phosphorylation or furin cleavage of ADAM17. Biochim. Biophys. Acta *1833*, 3355–3367.

Skovronsky, D.M., Fath, S., Lee, V.M.-Y., and Milla, M.E. (2001). Neuronal localization of the TNFalpha converting enzyme (TACE) in brain tissue and its correlation to amyloid plaques. J. Neurobiol. *49*, 40–46.

Sommer, A., Kordowski, F., Büch, J., Maretzky, T., Evers, A., Andrä, J., Düsterhöft, S., Michalek, M., Lorenzen, I., Somasundaram, P., et al. (2016). Phosphatidylserine exposure is required for ADAM17 sheddase function. Nat. Commun. *7*.

Sommer, A., Düppe, M., Baumecker, L., Kordowski, F., Büch, J., Fuchslocher Chico, J., Fritsch, J., Schütze, S., Adam, D., Sperrhacke, M., et al. (2017). Extracellular sphingomyelinase activity impairs TNF-α-induced endothelial cell death via ADAM17 activation and TNF receptor 1 shedding. Oncotarget *8*, 72584–72596.

Tobinick, E. (2009). Tumour Necrosis Factor Modulation for Treatment of Alzheimer ' s Disease Rationale and Current Evidence. *23*, 713–725.

Tomita, T. (2017). Aberrant proteolytic processing and therapeutic strategies in Alzheimer disease. Adv. Biol. Regul. *64*, 33–38.

Wang, W., Tan, M., Yu, J., and Tan, L. (2015). Role of pro-inflammatory cytokines released from microglia in Alzheimer's disease. Ann. Transl. Med. *3*, 1–15.

Xu, J., Mukerjee, S., Cristiane, C.R., Carvalho-Galvï¿½o, A., Cruz, J.C., Balarini, C.M., Braga, V.A., Lazartigues, E., and Franï¿½a-Silva, M.S. (2016). A disintegrin and metalloprotease 17 in the cardiovascular and central nervous systems. Front. Physiol. *7*, 1–14.

Xu, P., Liu, J., Sakaki-Yumoto, M., and Derynck, R. (2012). TACE activation by MAPK-mediated regulation of cell surface dimerization and TIMP3 association. Sci. Signal. *5*.

Zhang, F., and Jiang, L. (2015). Neuroinflammation in Alzheimer ' s disease. Neuropsychiatr. Dis. Treat. *11*, 243–256.

Zhao, M., Cribbs, D.H., Anderson, A.J., Cummings, B.J., Su, J.H., Wasserman, A.J., and Cotman, C.W. (2003). The induction of the TNFalpha death domain signaling pathway in Alzheimer's disease brain. Neurochem. Res. *28*, 307–318.

Zunke, F., and Rose-John, S. (2017). The shedding protease ADAM17: Physiology and pathophysiology. Biochim. Biophys. Acta - Mol. Cell Res. *1864*, 2059–2070.